Lawrence Berkeley National Laboratory
Lawrence Berkeley National Laboratory

Title
Implementation of the Barcelona Basic Model into TOUGH-FLAC for simulations of the geomechanical behavior of unsaturated soils

Permalink

Author
Rutqvist, J.

Publication Date
2010-06-26

Peer reviewed

IMPLEMENTATION OF THE BARCELONA BASIC MODEL INTO TOUGH-FLAC FOR SIMULATIONS OF THE GEOMECHANICAL BEHAVIOR OF UNSATURATED SOILS

Jonny Rutqvist[1, *], Yuji Ijiri[2], Hajime Yamamoto[2]

[1]Earth Sciences Division, Lawrence Berkeley National Laboratory, MS 90-1116, Berkeley, CA 947 20, USA

[2]Taisei Corporation, Nuclear Facility Division, 1-25-1 Nishi Shinjuku, Shinjuku, Tokyo 163-0606, Japan

* Corresponding author. Tel.: +1-510-486-5432, fax.: +1-510-486-5686
  e-mail address: jrutqvist@lbl.gov (J. Rutqvist)

June 2010

ABSTRACT

This paper presents the implementation of the Barcelona Basic Model (BBM) into the TOUGH-FLAC simulator analyzing the geomechanical behavior of unsaturated soils. We implemented the BBM into TOUGH-FLAC by (1) extending an existing FLAC^{3D} module for the Modified Cam-Clay (MCC) model in FLAC^{3D}, and (2) adding computational routines for suction-dependent strain and net stress (i.e., total stress minus gas pressure) for unsaturated soils. We implemented a thermo-elasto-plastic version of the BBM wherein the soil strength depends on both suction and temperature. The implementation of the BBM into TOUGH-FLAC was verified and tested against several published numerical model simulations and laboratory experiments involving the coupled thermal-hydrological-mechanical (THM) behavior of unsaturated soils. The simulation tests included modeling the mechanical behavior of bentonite-sand mixtures, which are being considered as back-fill and buffer materials for geological disposal of spent nuclear fuel. We also tested and demonstrated the use of the BBM and TOUGH-FLAC for a problem involving the coupled THM processes within a bentonite-backfilled nuclear waste emplacement tunnel. The simulation results indicated complex geomechanical behavior of the bentonite backfill, including a nonuniform distribution of buffer porosity and density that could not be captured in an alternative, simplified, linear-elastic swelling model. As a result of the work presented in this paper, TOUGH-FLAC with BBM is now fully operational and ready to be applied to problems associated with nuclear waste disposal in bentonite-backfilled tunnels, as well as other scientific and engineering problems related to the mechanical behavior of unsaturated soils.

1 INTRODUCTION

The Barcelona Basic Model (BBM) is a geomechanical constitutive model for capturing the elasto-plastic behavior of unsaturated soils. The model was first developed and presented in the early 1990s as an extension of the Modified Cam Clay (MCC) model to unsaturated soil conditions (Alonso et al., 1990). The model can describe many typical features of unsaturated-soil mechanical behavior, including wetting-induced swelling or collapse strains, depending on the magnitude of applied stress, as well as the increase in shear strength and apparent preconsolidation stress with suction (Gens et al., 2006).

In this paper, we present the implementation of the BBM into a coupled multiphase fluid flow and geomechanical simulator called TOUGH-FLAC (Rutqvist et al., 2002; Rutqvist, 2010). The TOUGH-FLAC simulator is based on the sequential coupling of a finite-difference geomechanical code, FLAC³ᴰ (Itasca, 2009) and a finite-volume, multiphase fluid flow code, TOUGH2 (Pruess et al., 1999). One great advantage of this approach to coupled-processes modeling is that both TOUGH2 and FLAC³ᴰ are being continuously developed and widely used, and therefore contain many constitutive and equation-of-state modules that can be readily applied to a wide range of scientific and engineering problems. In this case, we start with the existing MCC module in FLAC³ᴰ, which we then extend and modify to model the geomechanical behavior of unsaturated soil conditions within the framework of the BBM.

We implemented a thermo-elasto-plastic version of the BBM in which the soil strength depends on both suction and temperature, and includes features for expansive (swelling) clay (Gens, 1995). Figure 1 presents the three-dimensional yield surface in p'-q-s space and p'-q-T space, where p' is net mean stress (i.e., total stress minus gas-phase pressure), q is deviatoric stress (or shear stress), s is suction, and T is temperature (Gens, 1995). Under water-saturated conditions ($s = 0$), the yield

surface corresponds to the MCC ellipse (Roscoe and Burgland, 1968), and the size of the elastic

domain increases as suction increases. The rate of increase, represented by the loading-collapse (LC)

curve, is one of the fundamental characteristics of the BBM (Gens et al., 2006). Moreover, in the

thermo-elasto-plastic version of the BBM, the size of the yield surface decreases with temperature

(Figure 1). We implemented the BBM into TOUGH-FLAC by (1) extending an existing MCC

module within the framework of the FLAC^{3D} User Defined Model (UDM) capability, and (2) adding

computational routines for suction-dependent strains and net stress in unsaturated soils.

The thermo-elasto-plastic version of the BBM is also part of the CODE_BRIGHT finite element

code at the University of Cataluña, Barcelona (CIMNE, 2002, Olivella et al., 1996). It was recently

successfully applied to model the coupled thermal-hydrological-mechanical (THM) behavior of an

unsaturated bentonite clay associated with the FEBEX in situ heater test at the Grimsel Test Site,

Switzerland (Gens et al., 2009). The BBM has also been applied to other types of bentonite-sand

mixtures such as MX-80, considered as an option for an isolating buffer in the Swedish KBS-3

repository concept (Kristensson and Åkesson, 2008). TOUGH-FLAC with BBM is not intended to

be an improvement compared with CODE_BRIGHT, but it is an alternative to CODE_BRIGHT and

can be used for independent model analysis and verification of CODE_BRIGHT results, in particular

related to the geomechanical performance of bentonite-backfilled geological nuclear waste

repositories. Code-to-code verification may be the only option for checking and gaining confidence

in the modeling results that include complex, multiphase flow, coupled geomechanical phenomena.

In this paper, we first present the relevant equations of the thermo-elasto-plastic BBM, its relationship

to the MCC, and how it is implemented into TOUGH-FLAC. This is followed by the description and

results of a number of simulation tests to verify the implementation of the BBM in comparison to

published modeling, experimental, and laboratory data on THM behavior in unsaturated soils. Finally,

we test and demonstrate the use of TOUGH-FLAC with BBM for a problem related to geological

disposal of nuclear waste, involving the coupled THM performance of a bentonite back-filled nuclear waste deposition tunnel.

2   TOUGH-FLAC IMPLEMENTATION OF THE BBM

This section presents an overview of the thermo-elasto-plastic BBM and its implementation into TOUGH-FLAC. The description of the thermo-elasto-plastic BBM follows (in part) a continuum mechanics description of the BBM by Kristensson and Åkesson (2008) with an inclusion of temperature effects that originates from Gens (1995). The extension of the BBM to nonisothermal conditions in Gens (1995) was in turn based on pioneering work by Hueckel and co-workers, who developed a thermo-plastic constitutive model for saturated soils (Hueckel and Borsetto, 1990).

2.1   Stress state

We begin our description with the conventional (Terzaghi) effective stress that can be expressed as

$$\boldsymbol{\sigma}' = \boldsymbol{\sigma} - p^{\phi}\mathbf{I} \tag{1}$$

where $\boldsymbol{\sigma}'$ and $\boldsymbol{\sigma}$ are, respectively, the effective and total stress tensors (positive for compression), p^{ϕ} is pore pressure, and $\mathbf{I}$ is the identity tensor. The stress state can be divided into a hydrostatic part $(1/3)\text{trace}(\boldsymbol{\sigma}')\mathbf{I} = p'\mathbf{I}$ and deviatoric part $\mathbf{s} = \boldsymbol{\sigma}' - p'\mathbf{I}$, where p' is the effective mean pressure (or effective mean stress) that can be expressed explicitly as:

$$p' = p - p^{\phi} = \frac{1}{3}\left(\sigma_1 + \sigma_2 + \sigma_3\right) - p^{\phi} \tag{2}$$

where p is total mean pressure (total mean stress), and σ_1, σ_2, and σ_3 are principal compressive stresses. The conventional effective mean stress is used for water saturated conditions in the original MCC model (Roscoe and Burgland, 1968) as well as in the FLAC^{3D} implementation of MCC (Itasca, 2009). In the BBM, however, under unsaturated conditions, the strains are related to changes in two independent stress variables, namely the net mean stress for which

$$p' = p - p^g \tag{3}$$

and suction, s, is defined as

$$s = p^g - p^l \tag{4}$$

where p^g and p^l are gas- and liquid-phase pressures.

The deviatoric (von Mises) stress, q, is defined as:

$$q = \sqrt{3J_2} = \sqrt{3\frac{1}{2}\mathbf{s}\cdot\mathbf{s}} = \sqrt{\frac{\left(\sigma_1' - \sigma_2'\right)^2 + \left(\sigma_2' - \sigma_3'\right)^2 + \left(\sigma_1' - \sigma_3'\right)^2}{2}} \tag{5}$$

where J_2 is the second invariant of the effective deviatoric-stress tensor, $\mathbf{s}$.

For the implementation of the BBM into TOUGH-FLAC, both suction and gas pressure are needed. We calculated s from the TOUGH capillary pressure, which in turn is calculated from gas- and liquid-phase pressures according to Equation (4). Moreover, in TOUGH-FLAC, the concept of net mean stress for unsaturated soils is implemented by transferring the maximum of the gas- or liquid-phase pressure from TOUGH to FLAC^{3D} according to

$$p^\phi = MAX(p^l, p^g) \tag{6}$$

This approach enables simulation of both saturated and unsaturated soils. Under single-fluid phase conditions, the first primary variable is p^g for single gas phase or p^l for single liquid phase. For two fluid phase conditions, the primary variable is gas pressure, which is greater than the liquid pressure. As a result, for fully liquid saturated conditions, the conventional effective stress applies according to Equation (2), whereas for unsaturated conditions, the mechanical behavior depends on the two stress variables net, stress and suction, defined in Equations (3) and (4).

2.2 Strains due to stress, temperature and suction

The strain tensor can—similarly to the stress tensor—be expressed as the sum of a hydrostatic part $(1/3)\mathrm{trace}(\boldsymbol{\varepsilon})\mathbf{I}=(1/3)\varepsilon_v\mathbf{I}$ and deviatoric part $\mathbf{e} = \boldsymbol{\varepsilon} - (1/3)\varepsilon_v\mathbf{I}$, where ε_v is the volumetric strain associated with change in net mean stress, p', and can be explicitly expressed as

$$\varepsilon_v = \left(\varepsilon_1 + \varepsilon_2 + \varepsilon_3\right) \tag{7}$$

where ε_1, ε_2, and ε_3 are principal strains.

An equivalent deviatoric strain, associated with distortion and changes in deviatoric stress q, may be defined as

$$\varepsilon_q = \frac{2}{3}\sqrt{3J_2'} = \frac{2}{3}\sqrt{3\frac{1}{2}\mathbf{e}\cdot\mathbf{e}} = \frac{2}{\sqrt{6}}\sqrt{\left(\varepsilon_1 - \varepsilon_2\right)^2 + \left(\varepsilon_2 - \varepsilon_3\right)^2 + \left(\varepsilon_3 - \varepsilon_1\right)^2} \tag{8}$$

where J_2' stands for stands for the second invariant of the deviatoric-strain tensor $\mathbf{e}$.

For nonisothermal behavior of unsaturated soils, we may partition the total incremental strain into elastic, plastic, suction, and thermal strains:

$$\mathrm{d}\boldsymbol{\varepsilon} = \mathrm{d}\boldsymbol{\varepsilon}^e + \mathrm{d}\boldsymbol{\varepsilon}^p + \mathrm{d}\boldsymbol{\varepsilon}^s + \mathrm{d}\boldsymbol{\varepsilon}^T \tag{9}$$

where the suction strain corresponds to the hydraulic strain term suggested by Kristensson and Åkesson (2008a) and represents the strain associated with changes in suction. Each of these types of strain are described in the following subsections.

2.2.1 Elastic Strain

The mechanical volumetric elastic strain increment is associated with changes in net mean stress $\mathrm{d}p'$ according to

$$\mathrm{d}\varepsilon_v^e = \frac{1}{K}\mathrm{d}p' \tag{10}$$

where the bulk modulus K is defined as

$$K = \frac{(1+e)p'}{\kappa_{ps}(s)} \tag{11}$$

in which the compressibility function $\kappa_{ps}(s)$ is defined empirically as

$$\kappa_{ps}(s) = \kappa_{ps0}\left[1 + s\alpha_{ps}\right] \tag{12}$$

and thus κ_{ps0} and α_{ps} are empirical material constants.

The deviatoric elastic strain increment is defined as

$$d\varepsilon_q^e = \frac{1}{3G}dq \tag{13}$$

where G may be obtained using a constant Poisson's ratio ν in

$$G = \frac{3(1-2\upsilon)}{2(1+\upsilon)}K \tag{14}$$

Thus, the equations for elastic mechanical strain indicate the dependency of bulk modulus on suction (and hence fluid saturation) in which dry clay can be significantly stiffer than water-saturated clay.

In current FLAC^{3D} MCC implementation, there is the option of either inputting a constant υ and calculate G from Equation (14) or using a constant G and calculating υ from Equation (14). When implementing the BBM, this approach can be readily extended into unsaturated conditions, in which K is governed by Equation (11). Thus, in the non-linear elastic behavior of the BBM we may either choose to have a constant G or υ and this choice makes a difference when trying to analyze experimental data.

2.2.2 Plastic Strain

The temperature- and suction-dependent loading collapse (LC) yield surface (Figure 1) bounds the elastic region according to

8

$$f_{LC} = \frac{q^2}{g_y(\theta)^2} - \frac{M^2}{g_y(\theta=0)^2}\left(p' + p_s(s,T)\right)\left(p_0(s,T) - p'\right) = 0 \qquad (15)$$

where θ is the Lode's angle, and the function $g_y(\theta)$ describes the shape of the yield surface in the deviatoric plane (Kristensson and Åkesson, 2008a). M is the constant slope of the critical state line (Figure 1), whereas

$$p_s(s,T) = p_{s0} + k_s s \exp[-\rho_s \Delta T] \qquad (16)$$

represents the increases in cohesion with suction and temperature change $\Delta T = T - T_0$,

where k_s and ρ_s are empirical material constants.

In Equation (15), the function

$$p_0(s,T) = p^c\left(\frac{p_{0T}^*(T)}{p^c}\right)^{[\lambda_{Ps0} - \kappa_{Ps0}]/[\lambda_{Ps} - \kappa_{Ps0}]} \qquad (17)$$

is the net mean yield stress (or apparent pre-consolidation stress) at current suction and temperature, where

$$P_{0T}^*(T) = P_0^* + 2\left(\alpha_1 \Delta T + \alpha_3 \Delta T |\Delta T|\right) \qquad (18)$$

is the temperature-dependent net mean yield stress (or pre-consolidation stress) at full saturation and

$$\lambda_{PS}(s) = \lambda_{PS0}\left((1 - r_\lambda)\exp(-\beta_\lambda s) + r_\lambda\right) \qquad (19)$$

is a compressibility parameter in virgin soil states at suction s. Equation (18) is discussed in Gens (1995) and originates from Hueckel and Borsetto (1990) considering a suction-dependent thermoelastic energy potential that results in a decrease of the pre-consolidation stress $p_{0T}^*(T)$ and an associated reduction of the yield surface with temperature (Figure 1). Equation (19) is yet another empirical relationship in which λ_{Ps} determines the shape of the LC yield surface, which increases in size with suction (Figure 1).

When the stress state is on the yield surface, the plastic strains are obtained from the plastic flow rule

$$d\varepsilon_P^P = d\Lambda \frac{\partial g}{\partial p'} \qquad (20a)$$

$$d\varepsilon_q^P = d\Lambda \frac{\partial g}{\partial q} \qquad (20b)$$

where $d\Lambda$ is the plastic multiplier obtained from the consistency condition $df_{LC} = 0$, and g_{LC} is the plastic potential defined by

$$g_{LC} = \frac{\alpha_a q^2}{g_y(\theta)^2} - \frac{M^2}{g_y(\theta=0)^2}(p' + p_s(s,T))(P_0(p_0^*,s) - p') \qquad (21)$$

where α_a is a parameter that gives rise to the nonassociative model, i.e. $g_{LC} \neq f_{LC}$.

In the implementation of the BBM in FLAC[3D], substantial extensions of existing MCC equations must be implemented and programmed for calculating the mechanical plastic strain. These extensions include considering the saturation and temperature dependency of many parameters in Equations (15) to (21) that define the shape of the LC yield surface, as well as extension to nonassociative plasticity.

The calculation of the plastic multiplier $d\Lambda$ in FLAC[3D] was modified to account for suction and temperature-dependent tensile strength $p_s(s, T)$ and apparent preconsolidation stress $p_0(s, T)$, as well as to account for the nonassociativity parameter, α_a. This modification involves the adapting equations within the FLAC[3D] elastic predictor-plastic corrector algorithm. In this algorithm, current stress increments are guessed by Hooke's law. These increments are then added to the stresses from the previous time step, and then corrected back to the yield surface if the calculated principal stresses violate the yield criterion (Itasca, 2009).

By substituting the yield function g_{LC} from Equation (21) into Equations (20a) and (20b), we obtain:

$$d\varepsilon_v^P = d\Lambda c_a, \text{ where } c_a = M^2\left(2p' - p_c + p_s\right) \tag{22a}$$

$$d\varepsilon_q^P = d\Lambda c_b, \text{ where } c_b = \alpha_a 2q \tag{22b}$$

The elastic strain increments in Equations (10) and (13) may be expressed as the total strain subtracted from the plastic strain, and then by substituting plastic strain with Equations (22a and 22b) we obtain

$$dp' = Kd\varepsilon_v^e = K(d\varepsilon_v - d\varepsilon_v^P) = K(d\varepsilon_v - d\Lambda c_a) \tag{23a}$$

$$dq = 3Gd\varepsilon_q^e = 3G(d\varepsilon_q - d\varepsilon_q^P) = K(d\varepsilon_q - d\Lambda c_b) \tag{23b}$$

The current stress may then be calculated as

$$p' = p_0' + dp' = p_0' + K(d\varepsilon_P - d\Lambda c_a) = p_{est}' + Kd\Lambda c_a \tag{24a}$$

$$q = q_0 + dq = q_0 + K(d\varepsilon_P - d\Lambda c_b) = q_{est} + Kd\Lambda c_b \tag{24b}$$

where p'_{est} and q_{est} are the estimated stresses obtained in the previous step, plus the current incremental elastic estimates. The value of the plastic multiplier $d\Lambda$ may now be defined by substituting Equations (24a) and (24b) in Equation (11), requiring that the new stress point be located on the yield surface ($f_{LC}(q, p') = 0$). Then,

$$a(d\Lambda)^2 + bd\Lambda + c = 0 \tag{25}$$

where

$$a = \left(MKc_a\right)^2 + \left(3Gc_b\right)^2 \tag{26a}$$

$$b = -\left[Kc_a c_a^e + \frac{3}{\alpha_a}Gc_b c_b^e\right] \tag{26b}$$

$$c = f\left(q_{est}, p'_{est}\right) \tag{26c}$$

Finally, FLAC^{3D} evaluates new stresses p' and q from Equations (24a) and (24b) using the expression for $d\Lambda$ corresponding to the root of Equations (25) and (26) with smallest magnitude. Equation (22) to (26) are similar to those derived for the FLAC^{3D} MCC model (Itasca, 2009), but c_a, c_b, and b contain additional terms and factors as a result of adding suction and temperature-dependent p_s and p_0, and the nonassociativity parameter, α_a.

2.2.3 Thermal Strain

Thermally induced strains are purely volumetric:

$$d\varepsilon_v^T = \left(\alpha_0 + 2\alpha_2 \Delta T\right) dT \tag{27}$$

where α_0 and α_2 are material parameters corresponding to a temperature-dependent volumetric thermal expansion coefficient. Equation (27) originates from the suction-dependent thermoelastic energy potential derived by Hueckel and Borsetto (1990) as summarized by Gens (1995) and implemented in CODE_BRIGHT. In our case, Equation (27) is implemented as a simple extension of the existing thermal strain capability in FLAC^{3D}.

2.2.4 Suction Strain

In analogy with thermally induced strains, the suction strain is purely volumetric:

$$d\varepsilon_v^s = \frac{1}{K^s} ds \tag{28}$$

in which we (similarly to Kristensson and Åkesson, 2008a) define K^s to be the suction bulk modulus

$$K^s = \frac{(1+e)(s + p_{atm})}{\kappa_{sp}(p',s)} \tag{29}$$

where κ_{SP} is a compressibility parameter for suction induced strain defined as

$$\kappa_{sp}(p',s) = \kappa_{sp0}\left(1 + \alpha_{sp} \ln \frac{p'}{P_{ref}}\right)\exp(\alpha_{ss}s) \tag{30}$$

which is a purely empirical relation that is determined by matching the observed swellings at different applied stresses and suctions.

Suction strain was added to TOUGH-FLAC in an analogous manner to treatment of thermal strain in FLAC^{3D}, by adding an equivalent mean stress increment according to

$$dp^s = Kd\varepsilon_v^s = \frac{K}{K^s}ds \tag{31}$$

This is implemented in FLAC^{3D} by adding increments to the normal stresses:

$$d\sigma_{xx}^s = \frac{K}{K^s}ds \tag{32a}$$

$$d\sigma_{yy}^s = \frac{K}{K^s}ds \tag{32b}$$

$$d\sigma_{zz}^s = \frac{K}{K^s}ds \tag{32c}$$

Both K and K^s are dependent on suction and mean net stress, according to Equations (11) and (29), and are calculated within the new FLAC^{3D} BBM module, whereas the stress increments are added in a separate routine using FISH, which is a programming capability attached to FLAC^{3D} (Itasca, 2009).

2.3   Evolution of specific volume

In the existing FLAC^{3D} implementation of the MCC model, the evolution parameter is the specific volume v, defined as,

$$v = \frac{V}{V^s} \tag{33}$$

where V^s is the volume of solid particles contained in a volume, V, of soil. The incremental relation between volumetric strain and specific volume is

$$d\varepsilon_v = \frac{dv}{v} \tag{34}$$

and an updated specific volume for a new step, $i + 1$, is calculated according to

$$v^{i+1} = v^i \left(1 - d\varepsilon_v\right)$$

Using algebraic considerations of volume change along pre-consolidation and swelling lines (Alonso et al., 1990), the initial value for specific volume v_i can be shown to be a functions of the initial net mean stress and calculated from

$$v_i = v^c - \lambda_{ps} \ln\left(\frac{p_{0T}^*}{p^c}\right) + \kappa_{PS} \ln\left(\frac{p_{0T}^*}{p_i'}\right) \tag{36}$$

where v^c is a material input value of the specific volume at the reference net mean stress p^c.

From the evolution of the specific volume, porosity, ϕ, and void ratio, e, are evaluated as

$$\phi = \frac{V^\phi}{V} = \frac{v-1}{v} \tag{37}$$

$$e = \frac{V^\phi}{V^s} = v-1 \tag{38}$$

where V^ϕ is the pore volume. When implementing the BBM into TOUGH-FLAC, these concepts are readily expanded into the unsaturated soil domain.

2.4 TOUGH-FLAC BBM module and input data

The thermo-elasto-plastic BBM was programmed in C++ and invoked into FLAC[3D] according to the UDM capability available in FLAC[3D]. The new C++ routine was compiled as a DLL file (dynamic link library) that can be loaded into FLAC[3D] whenever needed. The module is currently designed to be used in a coupled TOUGH-FLAC simulation, but could easily be modified for a stand-alone FLAC[3D] simulation, using the FLAC[3D] single-phase unsaturated fluid and heat flow capabilities. In a TOUGH-

FLAC implementation of the BBM, we also developed a few FISH routines, such as one for calculating suction strain.

The extension of the MCC model to unsaturated media and nonisothermal conditions adds to the complexity and the number of input parameters required. Five parameters are required to define the MCC model, and seven additional parameters are required for the BBM model. In the thermo-elasto-plastic version of the BBM implemented in this study, the failure surface also depends on the temperature, and total of twenty-one material parameters are possible. Discussions on how to determine these parameters from laboratory experiments are given in Alonso et al. (1990) and Gens (1995), and more recently in Kristensson and Åkesson (2008a). Frequently, the number of laboratory tests may be sparse, and some parameters may therefore be determined by model calibration. Kristensson and Åkesson (2008a) developed numerical tools in a Mathcad environment for a quick assessment of BBM parameters from laboratory experiments.

3   SIMULATION TESTS TO VERIFY THE BBM IMPLEMENTATION

A number of simulation tests were conducted to verify the implementation of the thermo-elasto-plastic BBM within the FLAC[3D] UDM framework. These included basic tests at saturated conditions for the standard FLAC[3D] MCC model (Itasca, 2009), and tests under unsaturated conditions of the BBM using published literature data. Table 1 summarizes a few examples of the small-scale simulation tests. AGJ1 and AGJ2 simulation tests examples enable comparison to analytical results of Alonso et al. (1990), whereas the K&Å1, K&Å2 and K&Å3 provide comparison to both independent model simulations and actual experimental data on MX-80 bentonite reported in Kristensson and Åkesson (2008a). The key simulation results from four of these tests are presented in Figure 2, as

described in the second column of Table 1. One of the experiments, the K&Å1, is presented in more detail because it shows important loading and unloading behavior, including nonassociative plasticity.

The K&Å1 test example involves a laboratory compression test at constant suction with comparison to experimental data of MX-80 bentonite, as presented by Kristensson and Åkesson (2008a, b). This test was conducted in an oedometer, consisting of a steel ring around a sample subjected to humidified air through filters on both sides (Kristensson and Åkesson, 2008b; Duek, 2007). Pistons and force transducers were placed axially above the sample and radially through the steel ring, allowing for measurements of both axial and radial stresses.

Kristensson and Åkesson (2008a) studied this experiment, evaluated the BBM parameters using their Mathcad tool and presented simulation results using the CODE_BRIGHT finite element code with BBM. In our model, we directly adopt the material parameter developed and used by Kristensson and Åkesson (2008a), because our main interest is to use these data to conduct a detailed code-to-code verification of the TOUGH-FLAC BBM implementation.

The laboratory experiment by Duek (2007) was conducted by first loading the sample with axial compressive stress from 0.18 MPa to 19.77 MPa, and subsequently unloading the sample to 1.0 MPa. The loading and unloading was performed under a constant confining compressive stress of 2.97 MPa and a constant suction of 28 MPa. Both the experimental and numerical results show a significant irreversible volumetric deformation as a result of plastic collapsing soils (Figure 3). Kristensson and Åkesson (2008a) evaluated the parameters, first determining elastic parameters at relatively low stress and then defining the yield surface and plastic model parameters. This included a pre-consolidation pressure tuned to 7.7 MPa and λ_{ps0} to 0.101. Finally, the nonassociativity parameter α_a was calibrated

to 0.72, to match the evolution of the radial stress during the unloading (Kristensson and Åkesson, 2008a).

Figure 3 shows that for the input parameters listed in Table 2—including the nonassociativity parameter α_a set to 0.72—an excellent agreement is achieved between TOUGH-FLAC simulation results and independent model data published in Kristensson and Åkesson (2008a). To illustrate the effect of the nonassociative plasticity, we also present the results of an alternative simulation using associative plasticity ($\alpha_a = 1.0$). Using associative plasticity ($\alpha_a = 1.0$) the simulation results deviates more significantly from the experimentally q-vs-p' and radial stress evolution. Thus, it is important to consider nonassociative plasticity to replicate the stress-strain behavior observed in the laboratory for this type of material, which necessitated our implementation of nonassociative plasticity.

4 SIMULATION TESTS USING TOUGH-FLAC WITH BBM AND SWELLING

The interaction of the TOUGH-FLAC simulator with the newly implemented thermo-elasto-plastic BBM and suction strain capability were tested using two example problems:

1) A laboratory swelling stress experiment.

2) A bentonite-backfilled horizontal nuclear waste emplacement tunnel.

The two examples are simulated using two options:

A) A linear elastic (LE) swelling model using a swelling strain that is linearly dependent on saturation changes.

B) A full BBM simulation with suction-dependent swelling.

The use of the LE swelling model example enabled a comparison of simulated results to simple analytical calculations to verify the implemented routines for TOUGH-FLAC modeling of suction strain, whereas modeling of the full BBM provides a check and demonstration of the applicability of the entire TOUGH-FLAC and BBM system. Table 3 lists thermal and hydraulic properties of the bentonite, which were derived in a previous study from experimental data or by model calibration (Rutqvist and Tsang, 2004; Alonso et al. 2005) for the modeling of the FEBEX in situ experiment. For the LE swelling model, only a few mechanical input parameters were needed (as described in Section 4.1). The input parameters for the BBM simulations were extracted from Gens et al. (2009) and represent BBM material parameters derived specifically for the bentonite buffer at the FEBEX experiment (Table 2, last column).

4.1 TOUGH-FLAC Simulation of a Laboratory Swelling Stress Experiment

Swelling pressure tests are conducted on fully confined samples wetted to full saturation. In this case, the experiments were conducted on bentonite material used in the FEBEX in situ experiment and part of the international collaborative project DECOVALEX (Alonso et al., 2005). For a dry density of 1.6 g/cm^3 and 65% initial saturation, a swelling pressure of about 5 to 6 MPa developed at full saturation in the swelling experiments (Alonso et al. 2005).

For the LE swelling model, the model input parameters can be determined analytically to achieve a desired maximum swelling stress of 5 MPa. In such a case, the bentonite is assumed to behave elastically, with a volumetric swelling and a swelling stress that depends on the changes in water saturation, ΔS_l, according to:

$$\Delta\sigma'_{sw} = 3K\Delta\varepsilon_{sw} = K\Delta S_l \beta_{sw} \tag{39}$$

18

where $\Delta\sigma'_{sw}$ is the induced swelling stress (an effective stress), K is the bulk modulus, and β_{sw} is a moisture swelling coefficient. For an average bulk modulus of 20 MPa, the appropriate moisture swelling coefficient can be calculated using Equation (39) as:

$$\beta_{sw} = \frac{\Delta\sigma'_{sw}}{3K\Delta S_l} = \frac{5\cdot10^6}{3\cdot20\cdot10^6\cdot0.35} = 0.238 \tag{40}$$

The swelling stress experiments is simulated using a 3D 20×20×20 mm model with 20 elements in the vertical direction (Figure 4). The model boundaries are fixed for displacement normal to the boundaries, which means that the model is fully confined from a mechanical viewpoint. The model is also hydraulically confined (no flow across boundaries) except at the bottom (water inlet) where a fully saturated condition and a slightly elevated gas pressure. are applied. The simulation is conducted for about 10 days under isothermal conditions at a temperature of 25°C. Figure 4 shows a plot of the saturation distribution after about 4 days.

In the simulation, the soil sample becomes practically fully saturated in about 10 days (Figure 5a). The compressive stress increases proportionally to the saturation, but does achieve a maximum value of about 5.56 MPa, higher than the expected 5 MPa (Figure 5b). The reason for a higher-than-expected stress is that gas is trapped in a hydraulically confined model, and gas pressure increases by about 0.5 MPa (from 0.1 to maximum 0.6 MPa), creating an additional poro-elastic stress increase of about 0.5 MPa (Figure 5b). The effect of gas pressure on stress can be eliminated by setting Biot's constant to zero ($\alpha_B = 0$). In such a case, the final stress is 5.12 MPa, i.e., exactly 5 MPa above the initial stress of 0.12 MPa (Figure 5b). This shows that the implemented routines for suction strain in TOUGH-FLAC work as intended.

The full BBM model simulation results in a swelling stress of 5.35 MPa, which is in agreement with experimental data and similar to the final swelling stress of the LE swelling model (Figure 5b).

However, a significant difference exists in the time evolution of stress in the results from the full BBM compared to those of the LE swelling model. The time evolution achieved in the case of the full BBM is the most realistic, because it accurately relates the volumetric change to changes in suction, in which most of the swelling takes place at high saturation values. In the case of the LE swelling model, the swelling is linearly related to saturation changes, but may be calibrated to achieve the correct final swelling pressure.

4.2   TOUGH-FLAC Simulation of a Bentonite-Backfilled Nuclear Waste Emplacement Tunnel

This modeling example is taken from the international DECOVALEX project involving a horizontal nuclear waste emplacement tunnel at 500 m depth (Rutqvist et al., 2008, 2009). Here, we present new model simulations of this example using TOUGH-FLAC to check and demonstrate the applicability of this coupled modeling approach to a problem involving complex, multimedia (canister, bentonite, rock) coupled THM interactions. The model simulation was conducted in a nonisothermal mode with a time-dependent heat power input over 100,000 years of simulation time (Figure 6). In this study we focus on the coupled THM behavior of the buffer, whereas the surrounding rock mass and its hydraulic and thermal properties affect the temperature and fluid pressure evolution. In this simulation, the rock permeability is sufficiently high (k = 1×10^{-17} m^2) so as to avoid suction-induced desaturation of the rock that could otherwise significantly affect the buffer resaturation (e.g., Rutqvist et al., 2005). The overall temperature evolution is controlled by the thermal decay function, assumed tunnel spacing (Figure 6), and rock-mass thermal properties. The rock thermal conductivity is set to 3 W/m°C, whereas the heat capacity is determined from a specific heat constant equal to 900 J/kg·°C, a 1% rock porosity, and a bulk density of 2700 kg/m^3 (Rutqvist et al., 2008). A direct code-to-code comparison of simulation results is provided using results from an independent numerical analysis with the finite element code ROCMAS (Rutqvist et al., 2001a).

Figure 7 presents the calculated evolution of temperature, saturation, fluid pressure, and stress within the buffer. The figure shows a good agreement between the simulation results of the TOUGH-FLAC and ROCMAS codes. The slight disagreement that can be observed in Figure 7 can be attributed to differences in the modeling approach. Indeed, ROCMAS is a finite element code for fully coupled THM analysis under single phase unsaturated flow conditions, whereas TOUGH-FLAC is based on the sequential coupling of a finite volume fluid flow code to a finite difference geomechanical code, but with full multiphase flow capability—see Wang et al., (2010), for a recent discussion on single-versus-multiphase fluid flow modeling approaches for this type of problem). The results in Figure 7 are also in general agreement with simulation results of other numerical models for the same DECOVALEX bench-mark test presented in Rutqvist et al. (2008, 2009).

Figure 7d is of utmost interest here because it shows the evolution of stress as a result of three sources: (1) swelling stress caused by saturation changes, (2) poro-elastic stress from fluid pressure changes under saturated conditions, and (3) thermal stress. The poro-elastic stress resulting from the restoration of fluid pressure accounts for about 4.5 MPa of total stress. Indeed, this contribution is proportional to the evolution of fluid pressure in Figure 7c. The swelling caused by saturation changes amounts to about 5 MPa, leading to a total stress change of 9.5 MPa. The contribution to the total buffer stress from the thermal expansion is about 0.4 MPa at the thermal peak. This is reasonable considering the magnitudes of temperature increase $\Delta T \approx 55°C$, a bulk modulus $K = 20$ MPa, and thermal expansion coefficient of $\alpha_T = 1.5 \times 10^{-4}$ °C^{-1}. A slight disagreement in the stress evolution at early times—during the first month of the 100,000 years simulation—can be attributed to differences in the modeling approach as previously mentioned. This is not surprising considering that the stress evolution depends on a number of simultaneous coupled processes associated with evolutions of saturation, fluid pressure and temperature. A number of international code-comparison studies including experimental data have indeed shown that

among the parameters in Figure 7a through d (temperature, saturation, fluid pressure and stress), the stress evolution is the most difficult to model and consistently predict (e.g. Rutqvist et al., 2001b, Börgesson et al., 2005; Chijimatsu et al., 2009).

Figure 8 and 9 present the geomechanical results for TOUGH-FLAC simulations employing the thermo-elasto-plastic BBM with the material parameters representing the bentonite buffer taken from Gens et al. (2009), used for modeling of the FEBEX in situ heater experiment. Figure 8a shows that the stress evolution is relatively uniform within the buffer; the stress evolution near the canister (point V1) follows the stress evolution near the rock wall (point V2). The stresses at V1 and V2 increase and peak at about 8 to 9.5 MPa, but then decrease to about 6.5 to 7.5 MPa towards the end of the simulation. A stress peak of about 9.5 MPa could be expected as a result of the combined effect of swelling and pressure restoration, consistent with the results of the linear swelling model in Figure 7d. The relatively strong reduction in stress towards 100,000 years in Figure 8a is a result of cooling shrinkage at the time when the buffer has become relatively stiff. Indeed, Figure 8a also shows that the bulk modulus increases with stress and is affected by suction changes. The initial bulk modulus is about 2 MPa and peaks at about 200 MPa (0.2 GPa), i.e., a 100-fold increase in stiffness.

Figure 8b shows the evolution of porosity. A nonuniform porosity evolution can be observed with decreasing porosity at the canister (point V1) and increasing porosity at the rock wall (point V2). The porosity decreases near the canister as a result of drying and suction, which tends to contract the buffer. Meanwhile, the porosity increases near the buffer-rock interface as a result of wetting, which tends to expand the buffer. Interestingly, the porosity change occurring during the first few years never recovers even after full saturation and restoration of fluid pressure. The porosity does not recover because the buffer becomes stiff with the stress increases occurring after the first few years.

Figure 9 shows that at the end of the simulation, a nonuniform dry density is obtained that is consistent with the nonuniform porosity distribution. The nonuniformity of the buffer density is a result of the complex nonlinear elastic behavior and interactions of the outer and inner parts of the buffer. As described above, the porosity and therefore also buffer density does not recover because the buffer becomes stiff with the stress increases occurring after the first few years. This is an eye-opening result, one which warrants further detailed studies and confirmation with independent models and experiments that are out of the scope of this paper. In the FEBEX in situ experiment, the density and porosity indeed became non-uniform towards the end of the test, but in that case the buffer was still partially unsaturated (Gens et al., 2009). However, we conclude from this study that the mechanical evolution of the buffer is far more complex than what could be captured with the LE swelling model. The BBM implementation into TOUGH-FLAC provides a practical tool for a more realistic and rigorous analysis of the mechanical behavior associated with bentonite back-filled nuclear waste repository tunnels.

5   CONCLUDING REMARKS

A thermo-elasto-plastic constitutive model based on the Barcelona Basic Model (BBM) for mechanical behavior of unsaturated soils has been implemented into TOUGH-FLAC. The model has been tested using a number of simulation examples, both with regard to its implementation using the FLAC[3D] user defined model capability and with regard to modeling of suction-induced swelling in TOUGH-FLAC. The test simulations included comparison to both independent calculation results and experimental data from bentonite-sand mixtures considered for use in back-fill and protective buffers around disposed spent nuclear fuel in geological nuclear waste repositories. Excellent agreement was achieved between TOUGH-FLAC modeling results and independent analytical and numerical simulation results. Moreover, the TOUGH-FLAC with BBM was also tested on a full-scale nuclear waste repository problem involving the interaction of multiple components (buffer, canister, rock)

over a 100,000 year simulation time. The simulation indicated complex geomechanical behavior of the bentonite backfill, including a nonuniform distribution of buffer porosity and density that could not be captured in an alternative, simplified linear-elastic swelling model. The thermo-elasto-plastic BBM implemented into TOUGH-FLAC is now fully operational and ready to be applied to nuclear waste disposal and other scientific and engineering problems related to the geomechanical behavior of unsaturated soils. The TOUGH-FLAC with BBM is an alternative to CODE_BRIGHT, and is currently used in the Japanese and Swedish nuclear waste programs for independent model analysis and verification of complex coupled processes simulation results.

Future work will include an extension of the current BBM implementation in TOUGH-FLAC to more complete modeling of expansive clays, including double-structured behavior. In such an approach, the material consists of two structural levels: a microstructure in which interactions occur at particle level and a macrostructure that accounts for the overall arrangement of the material comprising aggregates and macropores (Gens et al. 2006, Sánchez et al., 2005, Gens and Alonso, 1992). Another possible development would be to consider the so-called SI (suction-induced) yielding, a feature that was included in the original study by Alonso et al. (1990). However, the SI yielding is not included in the current BBM implementation in CODE_BRIGHT at University of Cataluña, and neither was it considered in the recent study by Kristensson and Åkesson (2008a, b). According to Antonio Gens at University of Cataluña (personal communication, April 2009), the SI yield criterion has not been used in subsequent implementations because they were not completely satisfied with it. If one wants to consider plastic suction effects inside the main yield surface, it is preferable to go all the way to a double structured expansive model (e.g., Sánchez et al., 2005).

ACKNOWLEDGMENTS

NOTATIONS

c_a, c_b	=	Constants used in the calculation of the plastic multiplier [Pa]
e	=	Void ratio [-]
$\mathbf{e}$	=	Deviatoric strain tensor [-]
D_v	=	Effective molecular diffusion coefficient of vapor [m²/s]
f_{LC}	=	Yield surface for loading collapse in the BBM [Pa]
g_{LC}	=	Plastic potential for loading collapse in the BBM [Pa]
g_y	=	Parameter describing the shape of the yield surface in the BBM [-]
G	=	Shear modulus [Pa]
$\mathbf{I}$	=	Identity tensor (all components 0 except diagonals which are 1) [-]
k	=	Permeability [m²]
k_r	=	Relative permeability [-]
k_s	=	Parameter describing the increase of cohesion with suction in the BBM [-]
K	=	Bulk modulus [Pa]
K^s	=	Bulk modulus for suction induced volumetric strain in the BBM [Pa]
LC	=	Loading collapse yield surface in the BBM [-]
LC_i	=	Loading collapse yield surface at initial conditions in the BBM [-]
M	=	Slope of the critical state line in the BBM [-]
p	=	Total mean stress (Equation (2)), compression positive [Pa]
p'	=	Net mean stress (Equation (3)), compression positive [Pa]
p^c	=	A reference stress state for v-P' relation in virgin states in the BBM [Pa]
p_{est}	=	Estimated mean stress in FLAC³ᴰ elastic predictor-plastic corrector algorithm [Pa]
p^g	=	Gas phase, g, pressure [Pa]
p^l	=	Liquid phase, l, pressure [Pa]
p^ϕ	=	Pore pressure [Pa]
p_s	=	Tensile strength in the BBM [Pa]
p_{s0}	=	Tensile strength at saturated conditions in the BBM [Pa]
p_0	=	Net mean yield stress at current suction and temperature in the BBM [Pa]
p_{ref}	=	Reference stress state for relating elastic compressibility to suction in the BBM [Pa]
p_{0T}^*	=	Net mean yield stress for saturated conditions at reference temperature in the BBM [Pa]
r_λ	=	Parameter defining the maximum soil stiffness associated with LC yield in the BBM [-]

s	=	Suction [Pa]
$\mathbf{s}$	=	Deviatoric stress tensor [Pa]
S_l	=	Liquid phase saturation [-]
T_0	=	Reference temperature for temperature dependent cohesion in the BBM [°C]
T	=	Temperature [°C]
q	=	Deviatoric (von Mises) stress [Pa]
q_{est}	=	Estimated deviatoric stress in FLAC^{3D} elastic predictor-plastic corrector algorithm [Pa]
J_2	=	Second invariant of the effective deviatoric-stress tensor [Pa]
J'_2	=	Second invariant of the deviatoric-strain tensor [-]
v	=	Specific volume [-]
v_i, v_{ref}	=	Specific volume at initial and reference stress states [-]
V	=	Volume [m^3]
V^s	=	Volume of solid phase [m^3]
V^ϕ	=	Volume of pores [m^3]
α_a	=	Nonassociativity parameter in flow rule in the BBM [-]
α_B	=	Biot's effective stress coefficient [-]
α_{ps}	=	Parameter relating elastic compressibility to suction in the BBM [-]
α_{sp}	=	Parameter relating κ_{sp} to net mean stress in the BBM [-]
α_{ss}	=	Parameter relating κ_{sp} to suction in the BBM [-]
α_0, α_2	=	Parameters that relate elastic volumetric strain and temperature changes in the BBM [°C^{-1}]
α_T	=	Linear thermal expansion coefficient (equivalent to α_0) [°C^{-1}]
β_λ	=	Parameter for the increase of soil stiffness with suction in the BBM [Pa^{-1}]
β_{sw}	=	Moisture swelling coefficient in LE swelling model [-]
ε_v	=	Volumetric strain (=ε_{xx}+ ε_{yy}+ ε_{zz}) positive for contraction [-]
$\boldsymbol{\varepsilon}^s$	=	Suction strain tensor [-]
$\boldsymbol{\varepsilon}$	=	Total strain tensor [-]
$\boldsymbol{\varepsilon}^e$	=	Elastic strain tensor [-]
$\boldsymbol{\varepsilon}^p$	=	Plastic strain tensor [-]
$\boldsymbol{\varepsilon}^T$	=	Thermal strain tensor [-]
$\varepsilon_v^e, \varepsilon_q^e$	=	Elastic volumetric and deviatoric strains [-]
$\varepsilon_v^p, \varepsilon_q^p$	=	Plastic volumetric and deviatoric strains [-]
$\varepsilon_v^T, \varepsilon_v^s$	=	Thermal and suction induced volumetric strains [-]
ϕ	=	Porosity [-]
κ_{ps}	=	Compressibility parameter for elastic v-p' in the BBM [-]
κ_{ps0}	=	Initial (zero suction) slope for elastic v-p' in the BBM [-]
κ_{sp}	=	Compressibility parameter for suction-induced elastic strain in the BBM [-]
κ_{sp0}	=	κ_{sP} at reference stress P_{ref} and zero suction [-]
λ_{ps}	=	Compressibility parameter in virgin soil states at suction s in the BBM [Pa]
λ_{ps0}	=	Slope of v-p' relation in virgin soil states at zero suction in the BBM [Pa]
Λ	=	Plastic multiplier [-]
θ	=	Lode's angle [°]
ρ_d	=	Dry density, ρ_d [kg/m^3]
ρ_s	=	Parameter that relates cohesion to temperature in the BBM [-]
$\sigma_1, \sigma_2, \sigma_3$=		Principal compressive stress components [Pa]
$\boldsymbol{\sigma}$	=	Total stress tensor [Pa]
$\boldsymbol{\sigma}'$	=	Effective stress tensor [Pa]
ν	=	Poisson's ratio [-]

REFERENCES

Alonso E.E., Alcoverro, J., et al. (26 co-authors), 2005. The FEBEX benchmark test. Case definition and comparison of modelling approaches. International Journal of Rock Mechanics & Mining Sciences 42, 611-638.

Alonso, E.E., Gens, A., Josa, A., 1990. A constitutive model for partially saturated soils. Geotechnique 40, 405–430.

Börgesson, L., Chijimatsu, M., Nguyen, T.S., Rutqvist, J., Jing L. 2001. Thermo-hydro-mechanical characterization of a bentonite-based buffer material by laboratory tests and numerical back analyses. International Journal of Rock Mechanics & Mining Sciences 38, 105–127.

CIMNE, 2002. Code_Bright User's Guide, Part V1d Thermo-Elasto-Plastic Constitutiva Model. Departamento de Ingeniería del Terreno, Universidad Politécnica de Cataluña, Barcelona, Spain, 7pp.

Chijimatsu, M., Börgesson, L., Fujita, T., Jussila, P., Nguyen, S., Rutqvist, J., Jing, L., 2009. Model development and calibration for the coupled thermal, hydraulic and mechanical phenomena of the bentonite. Environmental Geology, 57, 1255–1261.

Dueck, A., 2007. Results from suction controlled laboratory tests on unsaturated bentonite – Verification of a model, In: Schanz, T. (Ed.) Experimental Unsaturated Soil Mechanics, Springer Proceedings in Physics 112, pp. 329–335.

Gens, A., 1995. Constitutive Laws, In: Gens, A., Jouanna, P., Schrefler, B.A. (Eds.) Modern Issues in Non-saturated Soils. Springer-Verlag, Wien, New York, pp. 129–158.

Gens, A, Alonso, E.E., 1992. A framework for the behaviour of unsaturated expansive clays. Canadian Geotechnical Journal 29, 1013–1032.

Gens, A., Sánchez, M., Guimarães, L. DO N., Alonso, E.E., Lloret, A., Olivella, S., Villar, M.V., Huertas, F., 2009. A full-scale in situ heating test for high-level nuclear waste disposal: observations, analysis and interpretation. Geotechnique 59, 1–23.

Gens, A., Sánchez, M., Sheng, D., 2006. On constitutive modelling of unsaturated soils. Acta Geotechnica 1, 137–147.

Hueckel, T., Borsetto, M., 1990. Thermoplasticity of saturated soils and shales. Constitutive equations. Journal of Geotechnical Engineering ASCE 116, 1765–1777.

Itasca, 2009. FLAC^{3D} V4.0, Fast Lagrangian Analysis of Continua in 3 Dimensions, User's Guide. Itasca Consulting Group, Minneapolis, Minnesota, 438pp.

Kristensson, O., Åkesson, M., 2008a, Mechanical modeling of MX-80 – Quick tools for BBM parameter analysis. Physics and Chemistry of the Earth 33, S508–S515.

Kristensson O., Åkesson M., 2008b, Mechanical modeling of MX-80 – Development of constitutive laws. Physics and Chemistry of the Earth 33, S504–S507.

Pruess, K., Oldenburg, C., Moridis, G., 1999. TOUGH2 User's Guide, Version 2.0, Report LBNL-43134, Lawrence Berkeley National Laboratory, Berkeley, California, 198pp.

Roscoe, K.H., Burland, J.B., 1968. On the generalized stress-strain behaviour of the `wet' clay, In: Heyman, J., Leckic, F.A. (Eds.), Engineering Plasticity, Cambridge University Press, Cambridge, pp. 535–609.

Olivella, S., Gens, A., Carrera, J., Alonso, E.E., 1996. Numerical formulation for a simulator 'CODE_BRIGHT' for the coupled analysis of saline media. Engineering Computations 13, 87–112.

Rutqvist J., 2010. Status of the TOUGH-FLAC simulator and recent applications related to coupled fluid flow and crustal deformations. Computers and Geosciences (this issue).

Rutqvist, J, Barr, D., Birkholzer, J.T., Chijimatsu, M., Kolditz, O., Liu, Q., Oda, Y., Wang, W., Zhang, C., 2008. Results from an international simulation study on coupled thermal,

hydrological, and mechanical (THM) processes near geological nuclear waste repositories. Nuclear Technology 163, 101–109.

Rutqvist, J., Barr, D., Birkholzer, J.T., Fujisaki, K., Kolditz, O., Liu, Q.-S., Fujita, T., Wang, W., Zhang, C.-Y., 2009. A comparative simulation study of coupled THM processes and their effect on fractured rock permeability around nuclear waste repositories. Environmental Geology 57, 1347–1360.

Rutqvist, J., Chijimatsu, M., Jing, L., De Jonge, J., Kohlmeier, M., Millard, A., Nguyen, T.S., Rejeb, A., Souley, M., Sugita, Y., Tsang, C.F., 2005. Numerical study of the THM effects on the near-field safety of a hypothetical nuclear waste repository – BMT1 of the DECOVALEX III project. Part 3: Effects of THM coupling in fractured rock. International Journal of Rock Mechanics & Mining Sciences 42, 745–755.

Rutqvist, J., Tsang, C.-F., 2004. A fully coupled three-dimensional THM analysis of the FEBEX in situ test with the ROCMAS code: prediction of THM behavior in a bentonite barrier, In: Stephansson, O., Hudson, J.A., Jing, L., (Eds.) Coupled T-H-M-C Processes in Geo-Systems: Fundamentals, Modelling, Experiments and Applications. Elsevier Geo-Engineering Book Series, Oxford, p. 143–148.

Rutqvist, J., Wu, Y.-S., Tsang, C.-F., Bodvarsson, G., 2002. A modeling approach for analysis of coupled multiphase fluid flow, heat transfer, and deformation in fractured porous rock. International Journal of Rock Mechanics & Mining Sciences 39, 429-442.

Rutqvist J., Börgesson L., Chijimatsu M., Kobayashi A., Nguyen T. S., Jing L., Noorishad J., Tsang C.-F., 2001a. Thermohydromechanics of Partially Saturated Geological Media – Governing Equations and Formulation of Four Finite Element Models. International Journal of Rock Mechanics & Mining Sciences 38, 105–127.

Rutqvist J., Börgesson L., Chijimatsu M., Nguyen T. S., Jing L., Noorishad J., and Tsang C.-F. 2001b. Coupled Thermo-hydro-mechanical Analysis of a Heater Test in Fractured Rock and Bentonite at Kamaishi Mine – Comparison of Field Results to Predictions of Four Finite Element Codes. International Journal of Rock Mechanics & Mining Sciences 38, 129–142.

Sánchez, M., Gens, A., Guimarães, L. do N., Olivella, S., 2005. A double structure generalized plasticity model for expansive materials. International Journal of Numerical and Analytical Methods in Geomechanics 29, 751–787.

van Genuchten, MT., 1980. A closed-form equation for predicting the hydraulic conductivity of unsaturated soils. Soil Sciences Society of America Journal 44, 892–898.

Wang, W., Rutqvist, J., Görke, U.-J., Birkholzer, J.T., Kolditz, O., 2010. Non isothermal flow in low permeable porous media: A comparison of Richards' and two-phase flow approaches. Environmental Earth Sciences Environmental Earth Sciences, DOI 10.1007/s12665-010-0608-1.

Table 1. Description of a few of the simulation tests that have been conducted to verify the BBM implementation in TOUGH-FLAC.

Test and source	Description and Results
AGJ1 Swelling and collapse at increasing confining stress (Case 1 in Alonso et al., 1990).	Involves three different loading paths for inducing volumetric deformation by wetting at increasing confining stress (Figure 2a). In all three cases loading collapse is induced by the movements of the *LC* curve from its initial position *LCi* to its final position LC_H. TOUGH-FLAC results in Figure 2a agree with analytical results presented in Figure 11 of Alonso et al. (1990).
AGJ2 Swelling and collapse at alternate load paths (Case 2 in Alonso et al., 1990).	Volumetric deformation is induced along three alternate paths of mechanical loading and suction (Figure 2b). The different combinations of wetting and loading induce either expansion or collapse, but the final volumetric deformation is the same at the final position H. TOUGH-FLAC results in Figure 2b agree with analytical results presented in Figure 12 of Alonso et al. (1990).
K&Å1 Compression of MX-80 (Section 5.1 in Kristensson and Åkesson, 2008a).	A compression test with axial loading in steps followed by two unloading steps. The experiment provides the evolution of axial and the radial stresses as well as the void ratio. The TOUGH-FLAC modeling of this experiment is described in more detail in Section 4 and Figure 3.
K&Å2 Swelling of MX-80 under constant axial load (Section 5.2 in Kristensson and Åkesson, 2008a).	A swelling test subjected to a constant axial stress level. Wetting with associated suction decrease induces an increase in void ratio and compressive radial stress (Figure 2c). TOUGH-FLAC results are in agreement with modeling results and experimental data presented in Kristensson and Åkesson, (2008a).
K&Å3 Triaxial compression and shear of MX-80 (Section 5.3 in Kristensson and Åkesson, 2008a).	A triaxial experiment performed by applying an increasing axial strain to a test sample, while monitoring triaxial stress state and displacements (Figure 2d). TOUGH-FLAC results are in agreement with modeling results and experimental data presented in Kristensson and Åkesson, (2008a).

Table 2. Thermo-elasto-plastic BBM input parameters for simulation tests.

Parameter	AGJ1	AGJ2	K&Å1	K&Å2	K&Å3	FEBEX
κ_{PS0} (-)	0.02	0.02	0.057	0.06	0.1	0.05
κ_{SP0} (-)	0.008	0.008	0	0.3	0	0.25
G (MPa)	10	10	NA	NA	NA	NA
ν (-)	NA	NA	0.224	0.2	0.3	0.4
α_{SS} (-)	0	0	0	0	0	0
α_{PS} (MPa^{-1})	0	0	0	0	0	-0.003
α_{SP} (-)	0	0	0	0	0	-0.161
P_{ref} (MPa)	0.1	0.1	0	0.1	0	0.5
α_0 (°C^{-1})	0	0	0	0	0	1.5e-4
α_2 (°C^{-1})	0	0	0	0	0	0
λ_{PS0} (-)	0.2	0.2	0.101	0.9	0.135	0.15
R_λ (-)	0.75	0.75	0	0.75	0	0.925
β_λ (MPa^{-1})	12.5	12.5	0	0.03	0	0.1
ρ_s (°C^{-1})	0	0	0	0	0	0
k_s (-)	0.6	0.6	0.1	0.1	0.1	0.1
P_{S0} (MPa)	0	0	0	0	0	0
P^C (MPa)	0.1	0.1	0.1	0.2	0.1	0.5
M (-)	1	1	1	1	0.5	1
α_a (-)	0.4	0.4	0.72	1	0.5	0.53
v_λ (-)	2.033	2.033	2.140	4.173	2.135	1.937
P^*_0 (MPa)	0.2	0.6	7.7	3.5	1.5	12.0

Table 3. Thermal and hydraulic material parameters for the FEBEX buffer material used in the numerical modeling of swelling experiment and multiple barrier repository.

Parameter	Value/Function
Initial dry density, ρ_d [kg/m^3]	$1.6 \cdot 10^3$
Initial porosity, ϕ [-]	0.41
Saturated permeability, k [m^2]	$2.0 \cdot 10^{-21}$
Relative permeability, k_r [-]	$k_{rl} = S_l^3$
Van Genuchten's (1980) parameter, P_{VG} [MPa]	30
Van Genuchten's (1980) parameter, λ_{VG} [-]	0.32
Thermal expansion, β [1/°C]	$1.5 \cdot 10^{-4}$
Dry specific heat, C$_s$ [J/kg·°C]	$c_s = 1.38T + 732.5$
Thermal conductivity, λ_m [W/m·°C]	$\lambda_m = 1.28 - \dfrac{0.71}{1 + e^{(S_l - 0.65)/0.1}}$
Effective molecular diffusion coefficient, D_v [m^2/s]	$D_v = 2.16e - 5 \times \tau \times \phi \times S_g \left(\dfrac{T_{abs}}{273.8} \right)^{1.8}$
Mass flow times tortuousity factor, τ [-]	0.8
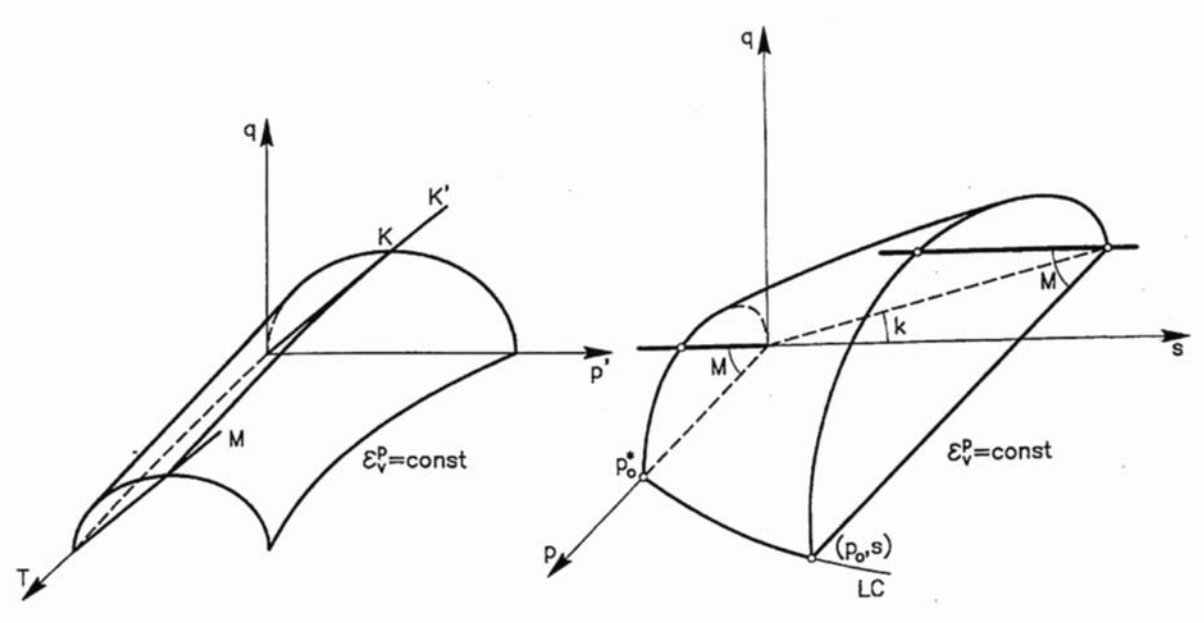
Figure 1. Three-dimensional representation of the yield surface in the thermo-elasto-plastic BBM (Gens, 1995).
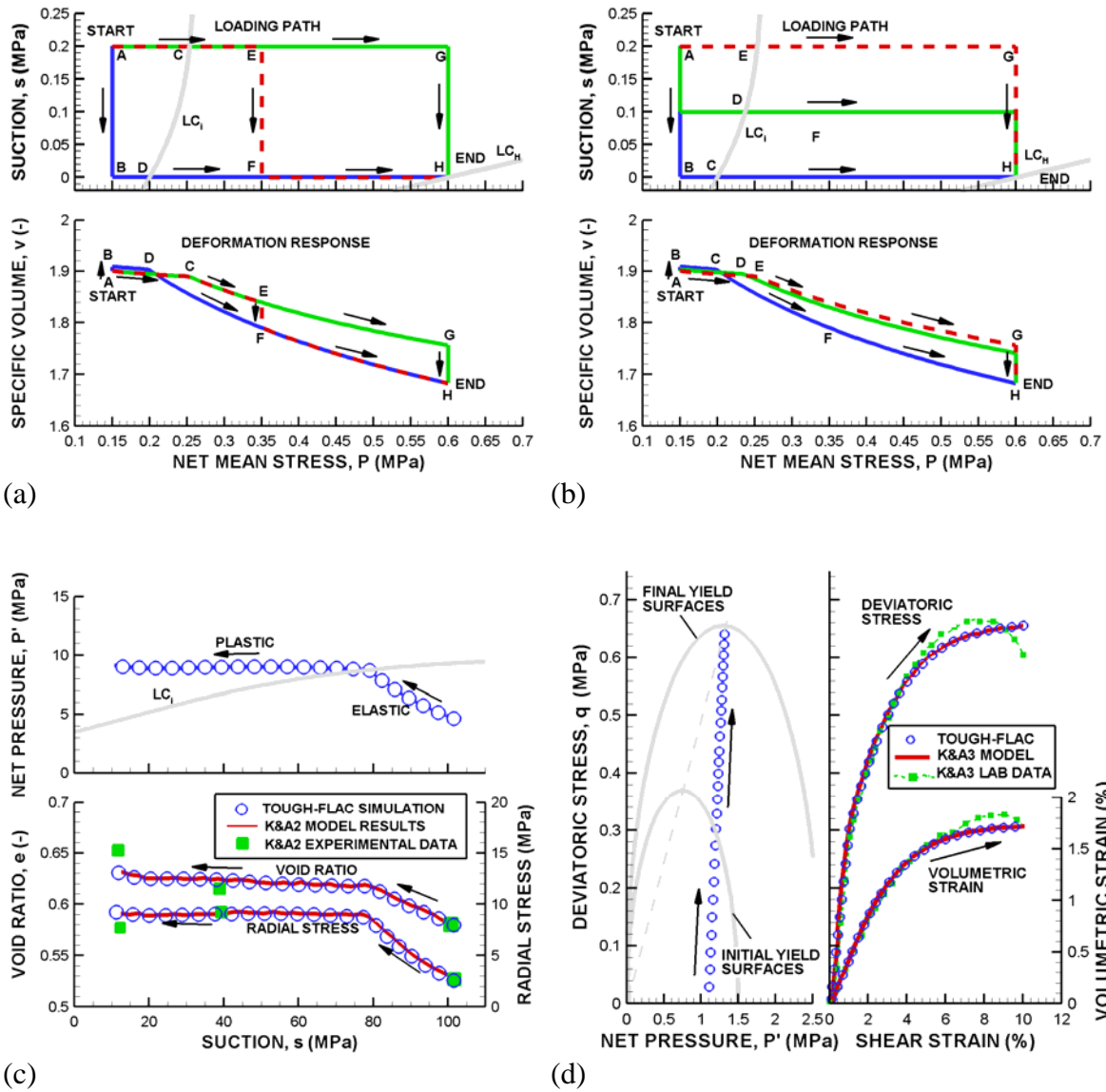
Figure 2. Result of simulation tests to verify the BBM implementation within the UDM capability of FLAC[3D]: (a) Swelling and collapse at increasing confining stress (AGJ1), (b) swelling and collapse at alternate load paths (AGJ2), (c) swelling of MX-80 under constant axial load (K&Å2), (d) triaxial compression and shear of MX-80 (K&Å3).
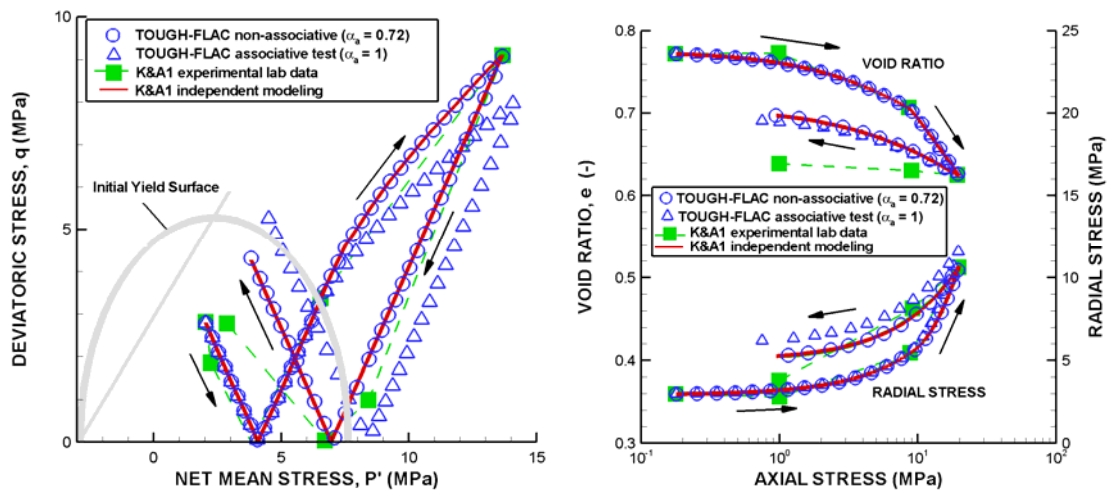
Figure 3. Comparison of TOUGH-FLAC with BBM simulation resultsl with experimental and modeling results presented in Kristensson and Åkesson (2008a) for MX-80 bentonite.
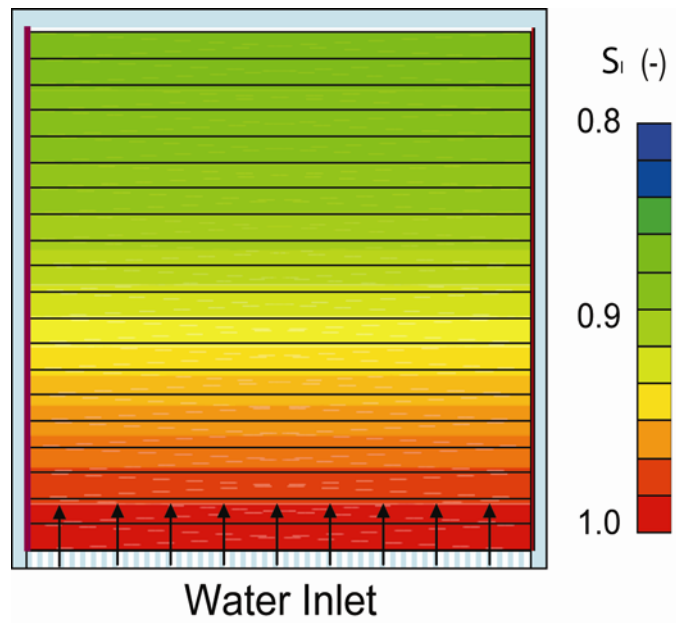
Figure 4.TOUGH-FLAC model of a swelling stress experiment and results of liquid saturation after 4 days of water infiltration.
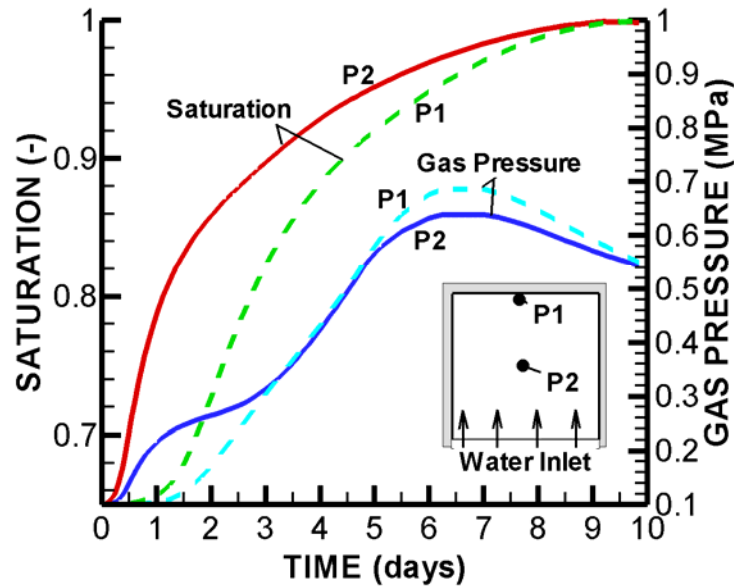
(a)
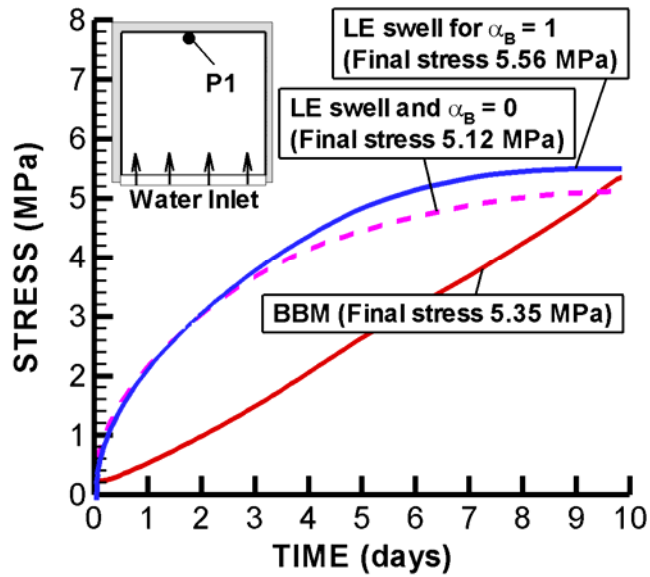
(b)

Figure 5. TOUHG-FLAC modeling of numerical swelling test: Simulated time evolution of (a) saturation and gas pressure at P1 and P2, and (b) stress at P1 for LE swelling model and BBM.
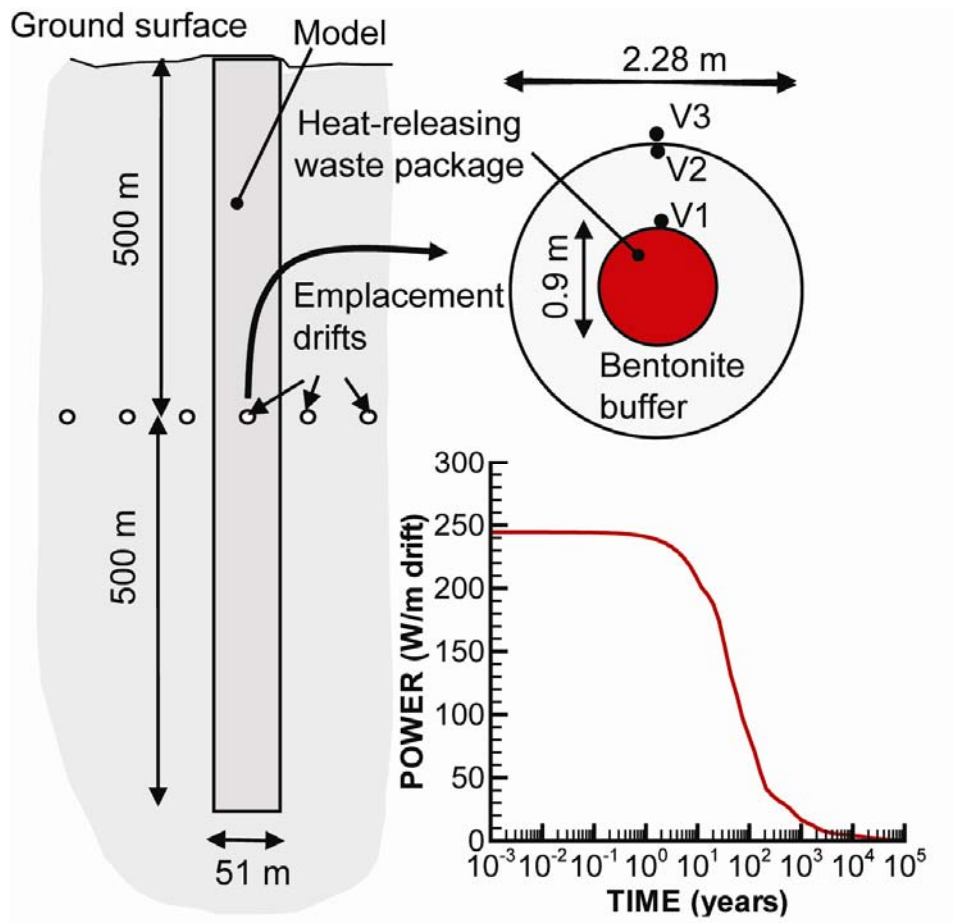
Figure 6. Model domain for a TOUGH-FLAC test example of a bentonite back-filled

horizontal emplacement drift at 500 m depth (Rutqvist et al., 2009).
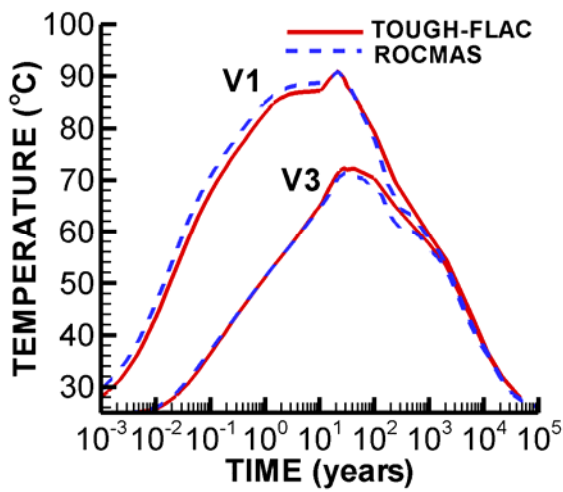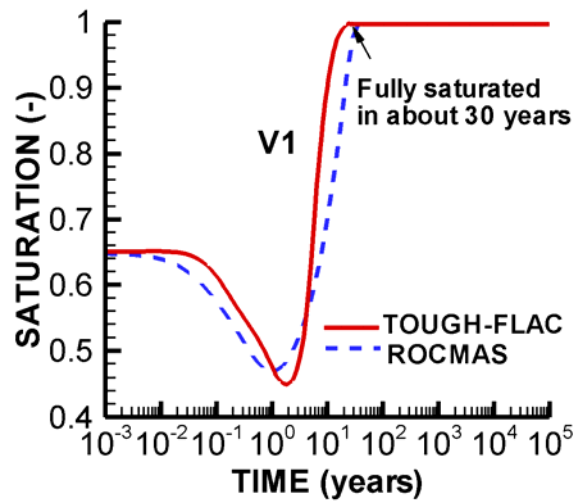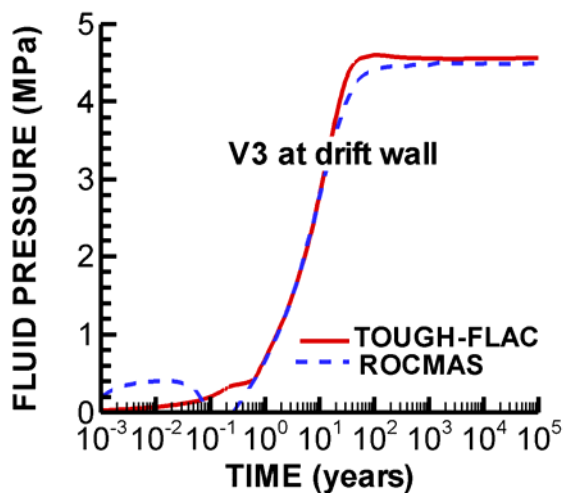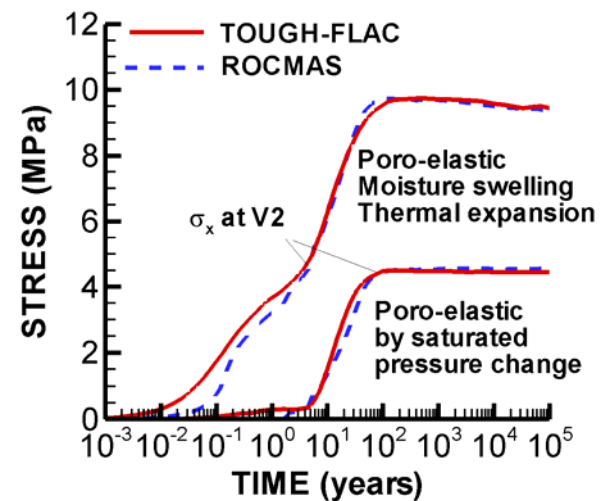
Figure 7. Simulated evolution of THM processes in the buffer: (a) temperature at V1 and V3, (b) liquid saturation at V1, (c) fluid pressure at V3, and (d) total radial stress (σ_x) at V2.
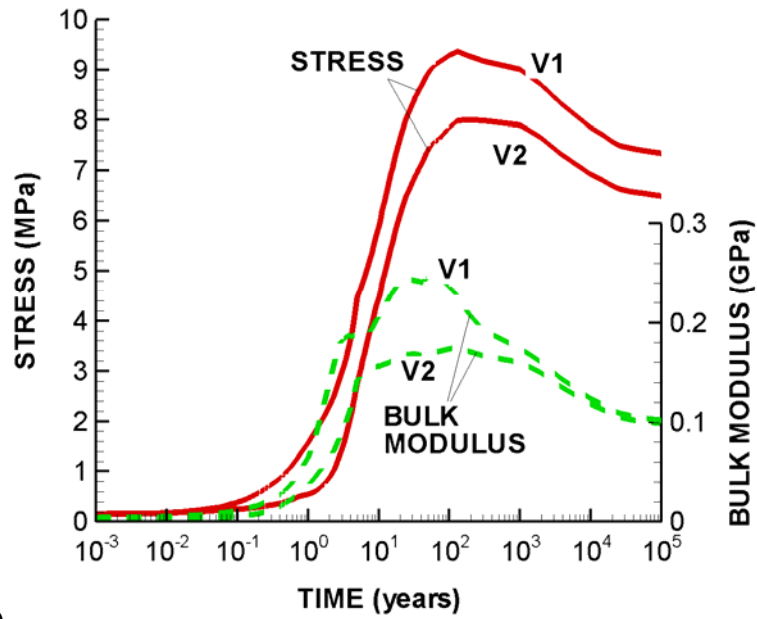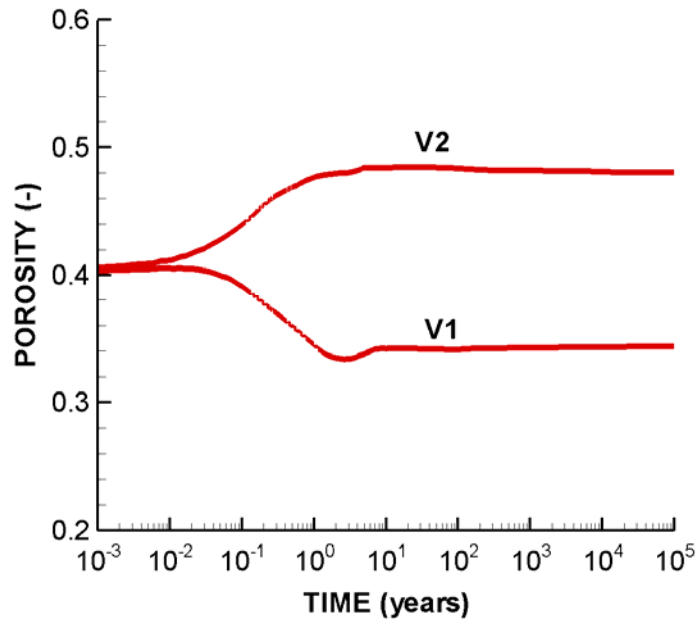
Figure 8. Simulated evolution of THM processes in the buffer when using the BBM: (a) tangential stress and bulk modulus, and (b) porosity for point V1 and V2 located within the buffer.
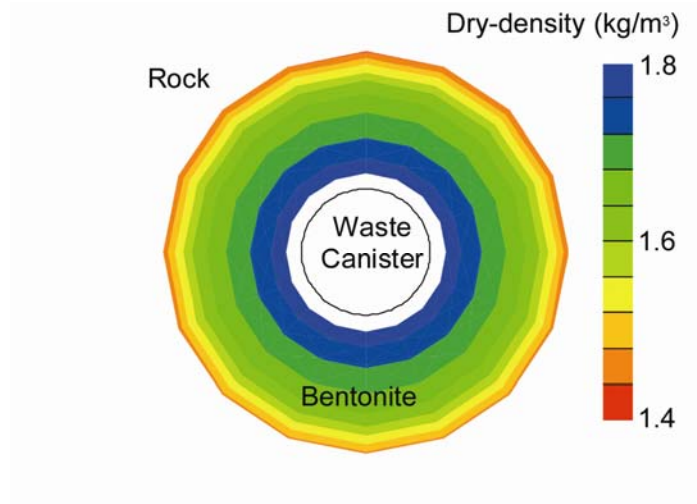
Figure 9. Calculated distribution dry-density in the buffer after full resaturation and restoration of ambient pressure and temperature (at 100,000 years) showing a relatively high density near the canister and a relatively low density near the rock wall.